Scattering at Rectangular-to-Rectangular Waveguide Junctions

REZA SAFAVI-NAINI AND ROBERT H. MACPHIE, SENIOR MEMBER, IEEE

Abstract—**This short paper presents formally exact solutions with convergent numerical results to the problems of scattering from a rectangular-to-rectangular waveguide junction and from a thick diaphragm with rectangular aperture in rectangular waveguide. The method uses normal mode expansions of the waveguide fields and the principle of conservation of complex power. A variety of configurations are considered and numerical convergence is confirmed by comparison with experiment.**

I. Introduction

For several decades the problem of electromagnetic scattering at the junction of two uniform cylindrical waveguides has attracted the attention of numerous authors. A survey of pertinent analytical and numerical techniques can be found in [1] and in texts by Mittra and Lee [2] and Lewin [3]. Transverse and longitudinal waveguide junctions may be considered as building blocks for more complex configurations such as filters, directional couplers, and periodic structures; consequently, in addition to their theoretical significance as boundary value problems, they are the key factors in the solution of many practical problems in microwave engineering.

Using normal TE- and TM-mode expansions for the waveguide fields, together with the principle of conservation of complex power [1], [4], this paper focuses on the junction of two rectangular waveguides with a common center axis but with otherwise arbitrary cross sections, and deduces its scattering matrix $\boldsymbol{S}$. The thick diaphragm with a centered rectangular hole can be regarded as a cascaded pair of such junctions. The overall scattering matrix $\boldsymbol{S}_d$ of such a structure is given in terms of generalized scattering matrix theory ([2], pp. 207–217) and the scattering matrices of the two junctions. The analysis, therefore, is quite different from the mode matching method of Luebbers and Munk [5], which uses even and odd excitations and, therefore, appears to be limited to the case where the waveguides on either side of the diaphragm are identical; moreover, an incomplete set of modes (no E_y) is postulated.

Numerical results are presented in Section III for a variety of junctions and diaphragms, while in Section IV a study of convergence reveals that quite good results are obtainable when about ten modes (TE plus TM) are used in the smaller of the two waveguides. Section V presents an experimental confirmation of the numerical results.

II. Method of Analysis

A. Rectangular-to-Rectangular Waveguide Junction

Fig. 1 illustrates a junction of two rectangular waveguides. The amplitude of the mnth scattered mode's electric field in waveguide i ($i=1,2$) due to a unit amplitude pqth mode in waveguide j ($j=1,2$) is by definition the (mn,pq) element of the field scattering matrix $\boldsymbol{S}_{ij}$. Moreover, for the smaller guide (guide 2)

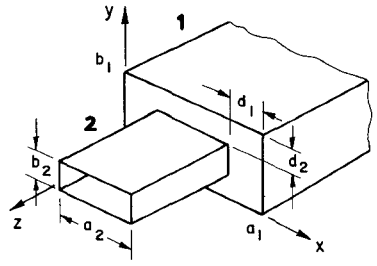

Fig 1. Junction of two rectangular waveguides.

$$\boldsymbol{S}_{22}=\boldsymbol{T}_2^{-1}(\boldsymbol{Y}_{02}+\boldsymbol{Y}_2)^{-1}(\boldsymbol{Y}_{02}-\boldsymbol{Y}_2)\boldsymbol{T}_2 \tag{1}$$

where $\boldsymbol{T}_i$ ($i=1,2$) is a diagonal matrix which defines the equivalent voltage column vector $\boldsymbol{V}_i$ of guide i in terms of the E-field mode amplitude vector $\boldsymbol{a}_i$ of the same guide

$$\boldsymbol{V}_i=\boldsymbol{T}_i\boldsymbol{a}_i. \tag{2}$$

$\boldsymbol{Y}_{02}$ is the characteristic admittance matrix of guide 2, and $\boldsymbol{Y}_2$ is the input admittance matrix of the junction as seen from guide 2. The principle of conservation of complex power can be used [1], [4] to show that

$$\boldsymbol{Y}_2=2\boldsymbol{T}_2^{-1\dagger}\boldsymbol{H}^{\dagger}\boldsymbol{P}_1^{\dagger}\boldsymbol{H}\boldsymbol{T}_2^{-1} \tag{3}$$

where $\boldsymbol{P}_1$ is a diagonal matrix whose mnth diagonal element is the complex power carried by the unit amplitude mnth mode of guide 1. The elements of H are given by [4]

$$H_{mn,pq}=Y^*_{01,mn}\frac{\iint_{S_a}\vec{e}_{1,mn}\cdot\vec{e}_{2,pq}\,da}{p_{1,mn}} \tag{4}$$

where $\vec{e}_{i,mn}$ ($i=1,2$) is the transverse component of the mnth mode electric field of guide i at $z=0$, and $p_{i,mn}$ is the complex power carried by the same mode. Integration in (4) is over the junction's aperture S_a.

The remaining submatrices of the scattering matrix $\boldsymbol{S}$ can be obtained in terms of $\boldsymbol{S}_{22}$ [1], [4]

$$\boldsymbol{S}_{12}=\boldsymbol{H}(\boldsymbol{I}+\boldsymbol{S}_{22}) \tag{5}$$

$$\boldsymbol{S}_{21}=\boldsymbol{Q}_2^{-1}\boldsymbol{S}_{12}^T\boldsymbol{Q}_1 \tag{6}$$

$$\boldsymbol{S}_{11}=\boldsymbol{H}\boldsymbol{S}_{21}-\boldsymbol{I}. \tag{7}$$

$\boldsymbol{Q}_i$ for $i=1,2$ is a diagonal matrix whose mnth diagonal element is $\iint\vec{e}_{i,mn}\times\vec{h}_{i,mn}\cdot\vec{da}$ with the integration taken over the cross-sectional area of waveguide i; in lossless cases $\boldsymbol{Q}_i=\boldsymbol{P}_i^*$. $\boldsymbol{I}$ is the identity matrix.

Let the modes in each waveguide be divided into TE and TM modes and sequentially ordered. The matrix $\boldsymbol{H}$ can then be subdivided into four submatrices

$$\boldsymbol{H}=\begin{bmatrix}\boldsymbol{A} & \boldsymbol{B}\\ \boldsymbol{C} & \boldsymbol{D}\end{bmatrix} \tag{8}$$

where $\boldsymbol{A}$ and $\boldsymbol{D}$ give the cross coupling between the TE modes and TM modes in each waveguide and $\boldsymbol{B}(\boldsymbol{C})$ indicates the cross coupling between the TM(TE) modes in the smaller guide and the TE(TM) modes in the larger. Using the letters h and e to indicate

Manuscript received March 12, 1982; revised May 21, 1982. This work was supported by the Natural Sciences and Engineering Research Council (NSERC), Ottawa, Canada, under Grant A 2176.

R. Safavi-Naini was with the Department of Electrical Engineering, University of Waterloo, Waterloo, Ontario, N2L 3G1, Canada. He is now living in Tehran, Iran.

R. H. MacPhie is with the Department of Electrical Engineering, University of Waterloo, Waterloo, Ontario, N2L 3G1, Canada.

0018-9480/82/1100-2060$00.75 ©1982 IEEE

TE and TM modes respectively, the various elements of the diagonal matrices $\boldsymbol{Y}_{0i}$, $\boldsymbol{P}_1$, $\boldsymbol{Q}_i$ and $\boldsymbol{T}_2$, for rectangular waveguides, are

$$Y^h_{0i,mn} = \frac{\gamma_{i,mn}}{jk_0} Y_0 \quad Y^e_{0i,mn} = \frac{jk_0}{\gamma_{i,mn}} Y_0, \qquad i = 1,2 \tag{9}$$

$$p^h_{1,mn} = \frac{a_1 b_1}{2\epsilon_m \epsilon_n} Y^{h*}_{01,mn} \quad p^e_{1,mn} = \frac{a_1 b_1}{8} Y^{e*}_{01,mn} \tag{10}$$

$$Q^h_{i,mn} = p^{h*}_{i,mn} \quad Q^e_{i,mn} = p^{e*}_{i,mn}, \qquad i = 1,2 \tag{11}$$

$$T^h_{2,mn} = \sqrt{\frac{a_2 b_2}{\epsilon_m \epsilon_n}} \quad T^e_{2,mn} = \sqrt{\frac{a_2 b_2}{4}}\, \epsilon_m = \begin{matrix} 1, m = 0 \\ 2, m \neq 0 \end{matrix} \tag{12}$$

where mn indicates the mnth mode in the waveguide, k_0 is the wavenumber and

$$\gamma^2_{i,mn} = \left(\frac{m\pi}{a_i}\right)^2 + \left(\frac{n\pi}{b_i}\right)^2 - k_0^2. \tag{13}$$

The (mn, pq)th elements of the four submatrices of $\boldsymbol{H}$ (see (4) and (8)), are conveniently represented as the elements of the following 2×2 matrix

$$\begin{aligned} \boldsymbol{H}_{mn,pq} &= \begin{bmatrix} A_{mn,pq} & B_{mn,pq} \\ C_{mn,pq} & D_{mn,pq} \end{bmatrix} \\ &= \begin{bmatrix} \frac{nq}{b_1 b_2} & \frac{np}{b_1 a_2} \\ \frac{mq}{a_1 b_2} & \frac{mp}{a_1 a_2} \end{bmatrix} I\left(\frac{m}{a_1}, \frac{p}{a_2}, \frac{n}{b_1}, \frac{q}{b_2}\right) \\ &\quad + \begin{bmatrix} \frac{mp}{a_1 a_2} & -\frac{mq}{a_1 b_2} \\ -\frac{np}{b_1 a_2} & \frac{nq}{b_1 b_2} \end{bmatrix} I\left(\frac{n}{b_1}, \frac{q}{b_2}, \frac{m}{a_1}, \frac{p}{a_2}\right) \end{aligned} \tag{14}$$

where

$$I\left(\frac{m}{a_1}, \frac{p}{a_2}, \frac{n}{b_1}, \frac{q}{b_2}\right) = \frac{4\pi^2}{a_1 b_1 k_{c1,mn} k_{c2,pq}} C\left(\frac{m}{a_1}, \frac{p}{a_2}\right) S\left(\frac{n}{b_1}, \frac{q}{b_2}\right) \tag{15}$$

with

$$C\left(\frac{m}{a_1}, \frac{p}{a_2}\right) = \begin{cases} \dfrac{m\pi}{a_1}\left[1 + (-1)^{m+p}\right] \dfrac{\sin\left[\frac{m\pi}{2a_1}(a_1 - a_2)\right]}{\left(\frac{m\pi}{a_1}\right)^2 - \left(\frac{p\pi}{a_2}\right)^2}, & \dfrac{m}{a_1} \neq \dfrac{p}{a_2} \\ \dfrac{a_1}{\epsilon_m}, & \dfrac{m}{a_1} = \dfrac{p}{a_2} \end{cases} \tag{16}$$

$$S\left(\frac{n}{b_1}, \frac{q}{b_2}\right) = \begin{cases} \dfrac{qb_1}{nb_2} C\left(\frac{n}{b_1}, \frac{q}{b_2}\right), & \dfrac{n}{b_1} \neq \dfrac{q}{b_2} \\ \dfrac{b_1}{2}, & \dfrac{n}{b_1} = \dfrac{q}{b_2} \end{cases}. \tag{17}$$

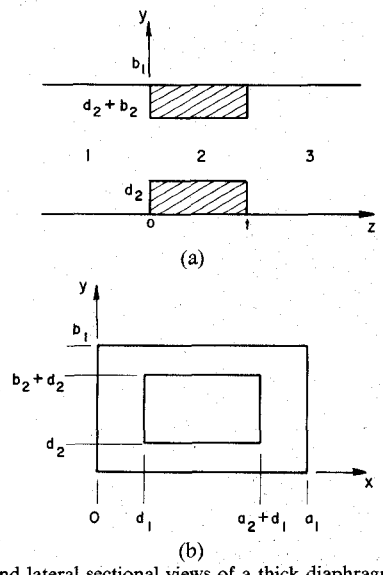

Fig. 2. Axial and lateral sectional views of a thick diaphragm with rectangular aperture.

Moreover, in (15)

$$k^2_{c1,mn} = \left(\frac{m\pi}{a_1}\right)^2 + \left(\frac{n\pi}{b_1}\right)^2, \quad k^2_{c2,pq} = \left(\frac{p\pi}{a_2}\right)^2 + \left(\frac{q\pi}{b_2}\right)^2. \tag{18}$$

It is interesting to note that by direct substitution of (15), (16), and (17) into (14) the submatrix $\boldsymbol{B}$ vanishes.

The use of (8)–(18) in (3) and (1) yields the desired scattering matrix $\boldsymbol{S}_{22}$ from which the three other scattering matrices are obtainable through (5), (6), and (7).

B. Diaphragm with Rectangular Aperture

Fig. 2 illustrates sectional views of the thick diaphragm. Applying the generalized scattering matrix technique ([2], pp. 207–217), which is valid for thin as well as thick diaphragms, one can obtain

$$\boldsymbol{S}^d_{11} = \boldsymbol{S}_{11} + \boldsymbol{S}_{12}\boldsymbol{L}\boldsymbol{S}_{22}\left(\boldsymbol{I} - \boldsymbol{L}\boldsymbol{S}_{22}\boldsymbol{L}\boldsymbol{S}_{22}\right)^{-1}\boldsymbol{L}\boldsymbol{S}_{21} \tag{19}$$

$$\boldsymbol{S}^d_{31} = \boldsymbol{S}_{12}\left(\boldsymbol{I} - \boldsymbol{L}\boldsymbol{S}_{22}\boldsymbol{L}\boldsymbol{S}_{22}\right)^{-1}\boldsymbol{L}\boldsymbol{S}_{21} \tag{20}$$

where the superscript d refers to the diaphragm and $\boldsymbol{L}$ is the diagonal transmission matrix of guide 2 with

$$L_{mn,mn} = \exp\{-\gamma_{2,mn} t\}. \tag{21}$$

The subscripts on the $\boldsymbol{S}_{ij}$ matrices indicate the scattering into the ith guide due to incident fields in the jth with $i, j = 1,2,3$. Accordingly, (19) gives the back scattering matrix for incidence from guide 1, and (20) is the forward scattering matrix for incidence from the same waveguide.

III. Numerical Results

The magnitude and phase of the reflection coefficient ρ and transmission coefficient τ, with incidence from the larger guide, are plotted in Fig. 3 as functions of frequency. These coefficients are the elements of $\boldsymbol{S}$ corresponding to a TE_{10} incident field and TE_{10} scattered fields. Since the characteristic admittance matrix elements are given by the mode admittances (see (9)), it turns out that $\boldsymbol{S}$ is nonsymmetric; moreover, as can be seen in Fig. 3, the transmission coefficient magnitude is (in this particular case) *greater* than unity, a result of the choice of admittance matrix elements. Note that the reflection coefficient magnitude in Fig. 3 is unity below 10.5 GHz since the smaller guide's TE_{10} mode is cut off below this frequency. Just above 10.5 GHz a sharp

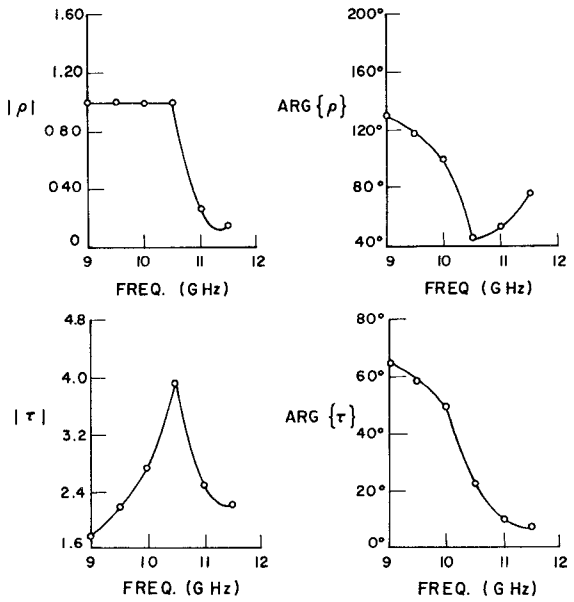

Fig. 3. Reflection coefficient ρ and transmission coefficient τ as functions of frequency with incidence from the larger waveguide. Dimensions of waveguides (in centimeters) are $a_1 = 2.285$, $b_1 = 1.005$, $a_2 = 1.428$, $b_2 = 0.650$.

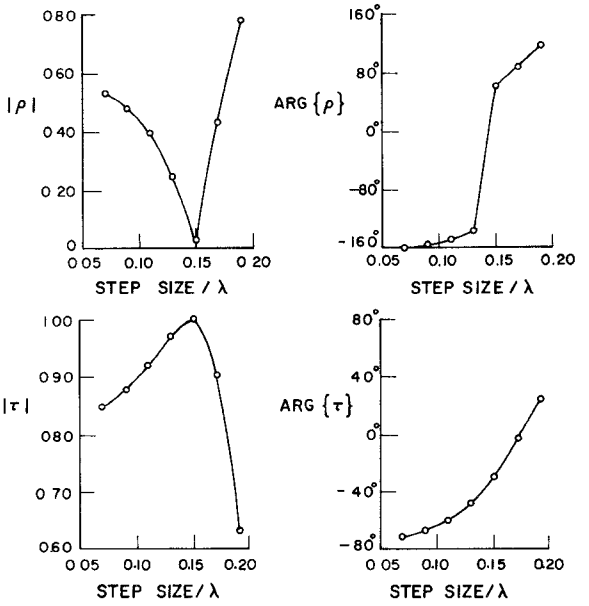

Fig. 5. Reflection coefficient ρ and transmission τ as functions of the step size d_1 in wavelengths for a thick diaphragm ($t = 0.25\lambda$). Waveguide dimensions are $a_1 = 0.85\lambda$, $b_1 = 0.40\lambda$, aperture height is $b_2 = 0.225\lambda$.

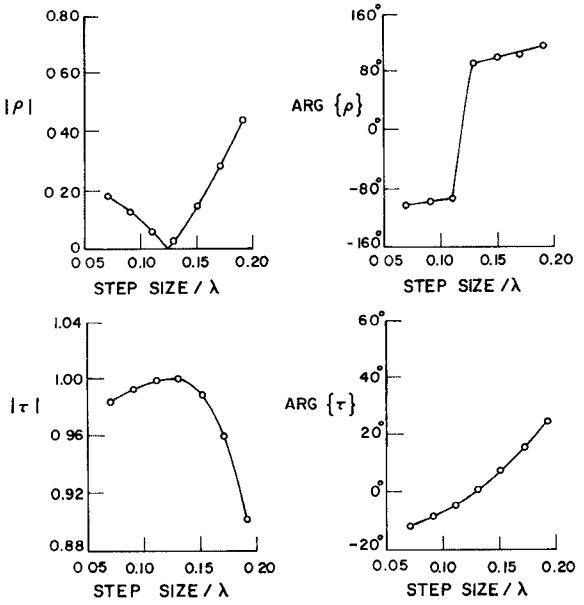

Fig. 4. Reflection coefficient ρ and transmission coefficient τ as functions of the step size d_1 in wavelengths for a thin diaphragm ($t = 0.01\lambda$). Waveguide dimensions are $a_1 = 0.85\lambda$, $b_1 = 0.40\lambda$, aperture height is $b_2 = 0.225\lambda$.

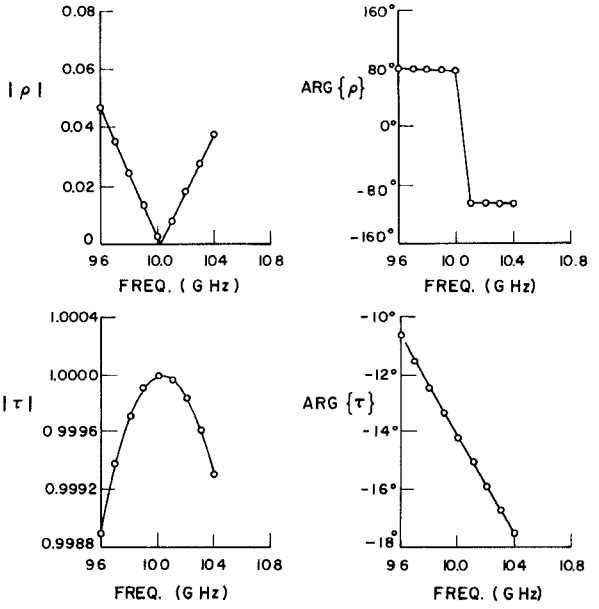

Fig. 6. Reflection coefficient ρ and transmission coefficient τ as functions of frequency for a thick diaphragm ($t = 0.25$ cm). Waveguide dimensions (in centimeters) are $a_1 = 2.285$, $b_1 = 1.005$, aperture dimensions are $a_2 = 1.800$, $b_2 = 0.660$.

decrease of $|\rho|$ signals the start of real power flow into guide 2.

Figs. 4 and 5, for the cases of two different thicknesses of a diaphragm with a centered rectangular iris, give the reflection coefficient ρ and transmission coefficient τ as functions of the step size in the x direction while the step size along y is held constant. With a TE_{10} incident mode field, the steps along x and y exhibit inductive and capacitive effects, respectively. When their reactances cancel one another, $|\rho|$ vanishes and the reflection coefficient angle becomes zero in its transition from negative to positive values. Due to the coupling between the two sides of the diaphragm, the location of the resonance point also depends on the thickness (compare Figs. 4 and 5). The thicker diaphragm introduces a higher selectivity due to the higher stored reactive energy. The standard formula for a resonant rectangular iris ([6, p. 170]) gives a value of step size d_1 which is 13 percent lower than that indicated by Fig. 4; for the thick iris, the formula, which is independent of thickness, is 27 percent lower than the value of $d_1 = 0.15\lambda$ given in Fig. 5. This discrepancy is, we feel, due to the simplicity of the standard formula which ignores the effects of all higher order modes and simply equates characteristic impedances of the TE_{10} modes in waveguides of cross sections $a_1 \times b_1$ and $a_2 \times b_2$, respectively.

The variation of the reflection coefficient ρ as a function of frequency is given in Fig. 6. The inductance and capacitance

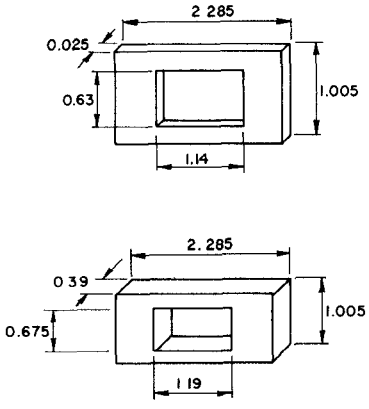

Fig 7. Diaphragms with rectangular apertures used in the experiments. Dimensions are in centimeters.

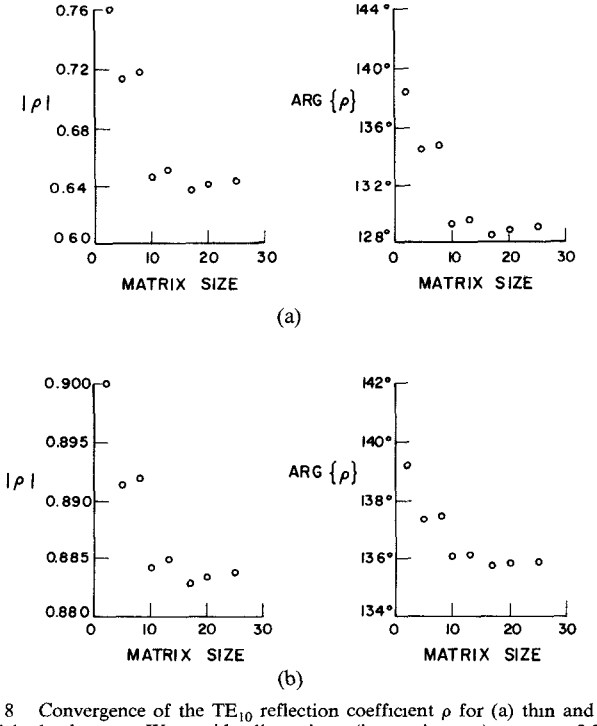

Fig. 8 Convergence of the TE_{10} reflection coefficient ρ for (a) thin and (b) thick diaphragms. Waveguide dimensions (in centimeters) are $a_1 = 2.285$, $b_1 = 1.005$, $f = 10.0$ GHz. (a) $t = 0.025$, $a_2 = 1.14$, $b_2 = 0.63$; (b) $t = 0.39$, $a_2 = 1\ 19$, $b_2 = 0.675$.

TABLE I
HIGHEST ORDER TE AND TM MODES CORRESPONDING TO EACH POINT OF FIG. 8

POINT NO	MATRIX SIZE	HIGHEST TE MODE	HIGHEST TM MODE
1	2	TE_{10}	TM_{12}
2	5	TE_{32}	TM_{12}
3	8	TE_{32}	TM_{34}
4	10	TE_{54}	TM_{12}
5	13	TE_{54}	TM_{34}
6	17	TE_{76}	TM_{12}
7	20	TE_{76}	TM_{34}
8	24	TE_{76}	TM_{56}

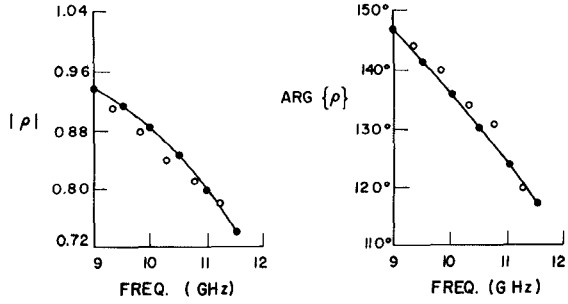

Fig. 9. Experimental and theoretical reflection coefficients as functions of frequency for thick diaphragm; experimental results are indicated by circles. Geometry is shown in Fig. 7(b).

introduced by the steps along x and y are frequency dependent, resonance occurring when their reactances cancel one another.

IV. Convergence

To examine the overall convergence of the technique, the magnitude and phase of the reflection coefficient ρ for the diaphragms shown in Fig. 7 are plotted in Fig. 8 as a function of the size of the matrix inverted in the computer program. The incident mode is TE_{10}. A list of the highest order smaller waveguide TE and TM modes corresponding to each point of the graphs is given in Table I.

V. Experiment

The magnitude and phase of the reflection coefficient ρ, i.e., $|\rho|$ and arg $\{\rho\}$, for the diaphragm shown in Fig. 7(b), were measured as functions of frequency. The results are superposed on the computed graphs in Fig. 9. It is seen that the results generated by the 10×10 matrix[1] inverted in the program are in good agreement with the measurements.

VI. Conclusions

Convergent results obtained in this paper for thick diaphragms in rectangular waveguide indicate the potential of the conservation of complex power technique. However, the analysis has only been applied to lossless structures. It will be of considerable interest to consider, say, the case of a resonant cavity formed by two diaphragms with rectangular apertures, and to take into account the finite conductivity of both the diaphragms and the waveguide walls.

Other configurations, such as the rectangular–circular waveguide junction and the coaxial-circular waveguide junction, are being investigated.

References

[1] R. Safavi-Naini, "On solving waveguide junction scattering problems by the conservation of complex power technique," Ph.D. thesis, University of Waterloo, Waterloo, Ontario, March 1979.
[2] R. Mittra and S. W. Lee, *Analytical techniques in the theory of guided waves*. New York: Collier–Macmillan, 1971.
[3] L. Lewin, *Theory of Waveguides*. New York: Halsted Press, John Wiley, 1975.
[4] R. Safavi-Naini and R. H. MacPhie, "On solving waveguide junction scattering problems by the conservation of complex power technique," *IEEE Trans. Microwave Theory Tech.*, vol. MTT-29, pp. 337–343, Apr. 1981.
[5] R. J. Luebbers and B. A. Munk, "Analysis of thick rectangular waveguide windows with finite conductivity," *IEEE Trans. Microwave Theory Tech.*, vol. MTT-21, pp 461–468, July 1973.
[6] C. G. Montgomery, R. H. Dicke, and E. M. Purcell, *Principles of Microwave Circuits*. New York: McGraw-Hill, 1948.

[1]The highest order smaller waveguide TE and TM modes are TE_{54} and TM_{12}.